

University of Wollongong Research Online

Australian Institute for Innovative Materials -
Papers

Australian Institute for Innovative Materials

1-1-2018

A contactless approach for monitoring the mechanical properties of swollen hydrogels

Andres Ruland Palaia
University of Wollongong, ruland@uow.edu.au

Xifang Chen
University of Wollongong, xc734@uowmail.edu.au

Afsaneh Khansari
University of Wollongong, ak569@uowmail.edu.au

Cormac Fay
University of Wollongong, cfay@uow.edu.au

Sanjeev Gambhir
University of Wollongong, sanjeev@uow.edu.au

See next page for additional authors

Follow this and additional works at: <https://ro.uow.edu.au/aiimpapers>

 Part of the [Engineering Commons](#), and the [Physical Sciences and Mathematics Commons](#)

Recommended Citation

Ruland Palaia, Andres; Chen, Xifang; Khansari, Afsaneh; Fay, Cormac; Gambhir, Sanjeev; Yue, Zhilian; and Wallace, Gordon G., "A contactless approach for monitoring the mechanical properties of swollen hydrogels" (2018). *Australian Institute for Innovative Materials - Papers*. 3276.
<https://ro.uow.edu.au/aiimpapers/3276>

Research Online is the open access institutional repository for the University of Wollongong. For further information contact the UOW Library: research-pubs@uow.edu.au

A contactless approach for monitoring the mechanical properties of swollen hydrogels

Abstract

Using a customized ultrasound setup we investigate the feasibility of using a contactless approach to study the bulk mechanical properties of swollen hydrogels. The study involved two different hydrogels, gelatin methacrylate (GelMa) and green algae extract methacrylate (GAEM), which were prepared to provide materials with varying modulus and different swelling properties. Two approaches have been developed. In the first case, ultrasound was compared to Young's modulus measured by indentation. It was found that can be linearly related to indentation modulus values only when the hydrogel swelling ratio is taken into account. In the second approach, an exponential dependency between swelled thickness and indentation modulus was found. This is representative for each hydrogel and purification method in addition to being independent of the conditions used within the toughness range explored. The results of this study indicate that a simple thickness measurement via the proposed approach can provide a direct relationship to Young's modulus upon calibration.

Disciplines

Engineering | Physical Sciences and Mathematics

Publication Details

Ruland , A., Chen, X., Khansari, A., Fay, C. D., Gambhir, S., Yue, Z. & Wallace, G. G. (2018). A contactless approach for monitoring the mechanical properties of swollen hydrogels. *Soft Matter*, 14 (35), 7228-7236.

Authors

Andres Ruland Palaia, Xifang Chen, Afsaneh Khansari, Cormac Fay, Sanjeev Gambhir, Zhilian Yue, and Gordon G. Wallace

DOI: 10.1002/ (adfm.201707520)

Article type: (Review)

Advances in Polar Materials for Lithium-Sulfur Batteries

Hongqiang Wang^{a,b,c}, Wenchao Zhang^b, Jianzhong Xu^a, Zaiping Guo^{b}*

Dr. H. Q. Wang, Prof. J. Z. Xu,
College of Chemistry & Environmental Science,
Hebei University,
Baoding, Hebei, 071002, PR China

Dr. H. Q. Wang, W. C. Zhang, Prof. Z.P. Guo,
Institute for Superconducting & Electronic Materials, School of Mechanical, Materials and
Mechatronics Engineering,
University of Wollongong,
Wollongong, NSW 2522, Australia
E-mail: zguo@uow.edu.au

Dr. H. Q. Wang
Fengfan Company Limited,
Baoding, Hebei, 071057, PR China

Keywords: lithium-sulfur batteries; polar inorganics; polar organics; chemical interaction.

Abstract Lithium-sulfur batteries are regarded as promising candidates for energy storage devices due to their high theoretical energy density. Various approaches have been proposed to break through the obstacles that are preventing Li-S batteries from realizing practical application. Recently, the importance of the strong chemical interaction between polar materials and polysulfides has been recognized by researchers to improve the performance of Li-S batteries, especially with respect to the shuttle effect. Polar materials, unlike nonpolar materials, exhibit strong interactions with polysulfides without any modification or doping because of their intrinsic polarity, absorbing the polar polysulfides and thus suppressing the notorious shuttle effect. The recent advances on polar materials for Li-S batteries are reviewed here, especially the chemical polar-polar interaction effects towards immobilizing dissolved polysulfides, and the relationship between the intrinsic properties of the polar materials and the electrochemical performance of the Li-S batteries are discussed. Polar materials, including polar inorganics in the cathode and polar organics as binder for Li-S

batteries are respectively described. Finally, future directions and prospects for polar materials used in Li-S batteries are also proposed.

1. Introduction

The rechargeable lithium-sulfur (Li-S) batteries have attracted enormous attention in the last several years due to their ultra-high theoretical specific capacity (1675 mAh g^{-1}) and energy density (theoretically 2567 Wh kg^{-1}),^[1-4] five times higher than for the traditional lithium-ion batteries. Sulfur cathodes still suffer, however, from low active material utilization and poor cycling stability due to several factors: (i) The low electrical conductivity of sulfur and its discharge products limit electron transport in the cathode; (ii) large volume changes in the sulfur upon lithiation disrupt the electronic integrity of the electrode; and (iii) high solubility of lithium polysulfide (Li_2S_n) species in organic electrolytes and the related “shuttle effect” lead to severe capacity fading, which is obstructing their practical application.^[5-9]

Tremendous efforts have been devoted to the complex problems listed above. In particular, early research was focused on the incorporation of sulfur into nonpolar carbon-based materials, including porous carbon, hollow carbon spheres, carbon nanotubes, graphene, and graphene oxide.^[10-23] The introduction of carbon-based materials serving as sulfur hosts could effectively ameliorate the issue of poor electrical conductivity and volume expansion during the charge-discharge process. On the other hand, in terms of chemical structure, polarity of molecule refers to a separation of electric charge, which results in an electric dipole or multipole in a molecule or its chemical groups. Because of the difference in electronegativity between the bonded atoms, the polar bonds must exist in the polar molecules. Polar molecules could interact through dipole–dipole intermolecular forces and hydrogen bonds. In general, the chemical interaction between two kinds of polar molecules is much stronger than that between a polar molecule and a nonpolar molecule. The Li_2S_n species belong to the class of polar molecules, while the carbon hosts are assigned to the nonpolar materials. Therefore, the

conjugate nonpolar carbon planes have limited sites to strongly anchor Li_2S_n species, resulting in weak interaction between the carbon-based materials and the Li_2S_n species. The nonpolar carbon based materials cannot effectively anchor polar polysulfides during cycling, especially over long-term cycling, so the issue of the shuttle effect still has not been solved.

Following this key point, the chemical affinity in polar-polar interaction is more favorable with respect to anchoring Li_2S_n species. Extensive work has been done on introducing polar sites onto carbon planes by heteroatom doping, such as O, N, S, and B doping, to enhance the interaction between Li_2S_n species and nonpolar carbon hosts.^[24-28] The doped sites and polar functional groups induced by heteroatom doping contribute to enhanced interaction between the carbon matrix and the polysulfides, effectively anchoring the polar sulfur species. The limited amount of doping and the number of polar sites, however, are still inadequate for the overall electrochemical performance of the Li-S batteries.

Recently, recognizing the importance of strong chemical interaction between polar materials and polysulfides, another stream of Li-S research has focused on exploring polar materials to trap polysulfides. Polar materials, unlike carbon materials, exhibit strong interaction with polysulfides without any modification or doping because of their intrinsic polarity, absorbing the polar polysulfides and thus suppressing the notorious shuttle effect. Herein, the polar materials used in Li-S batteries can be divided into two families. The first polar family mainly consists of inorganics, such as metal oxides, sulfides, carbides, and nitrides. Owing to their stronger interactions to bind polar polysulfides, many types of polar inorganics serve as efficient hosts to trap polysulfides. The second polar family mainly consists of organics, especially the newly developed polar binders used in Li-S batteries.

We summarize the recent advances in polar materials for Li-S batteries, including polar inorganic and polar organic materials. This review is organized into the following sections:

polar inorganics used in cathodes for Li-S batteries, polar organics used in binders for Li-S batteries, and the summary and outlook.

2. Polar inorganics used in cathodes for Li-S batteries

Polar inorganics used in cathode materials for Li-S batteries can be divided into two categories, additive materials and host materials. These materials share positive attributes that contribute to enhanced electrochemical performance of Li-S batteries. On the one hand, the polar inorganic materials possess a strong ability to absorb and trap polysulfides, thus avoiding the detachment of lithium polysulfides into the organic electrolyte, which significantly suppresses the shuttle effect. On the other hand, several polar materials in these inorganics are proven to accelerate the transformation process between lithium polysulfide and polysulfide due to their superior reactivity and abundant surface sites. All these features of polar inorganics endow Li-S batteries with improved reversibility, better stability, and longer lifetimes.

2.1 Polar additives materials

In early studies, nanosized $\text{Mg}_{0.6}\text{Ni}_{0.4}\text{O}$, Al_2O_3 , and La_2O_3 were firstly used as polar additives in carbon/sulfur cathode for the absorption of polysulfides, leading to improved coulombic efficiency and cycling stability.^[29-33] The polar metal oxide additives only can absorb a small amount of the polysulfides, however, due to their low surface area and relatively high density. To improve the absorption of the polar metal oxide additives, mesoporous α , β , and γ - TiO_2 with different surface areas and pore sizes were investigated by Nazar and coworkers for use in cathodes for Li-S batteries.^[34] The sulfur cathode fabricated with mesoporous carbon containing less than 4 wt% α - TiO_2 as additive demonstrated the highest capacity retention of 82% after 100 cycles. The Fourier transform infrared (FTIR) spectra and Raman spectra of α - TiO_2 /lithium polysulfide (LiPS) demonstrated the interaction between sulfur and titania (S-Ti-O bond, Figure 1a), which was the first report to prove the chemical interaction between a polar metal oxide and polysulfides. In order to effectively absorb the polysulfides and realize

high sulfur loading, a metal oxide additive with higher surface area was introduced into the sulfur/carbon cathode. Mesoporous SiO₂ with surface area of 850 m² g⁻¹ was used as an effective polysulfide reservoir material in CMK-3/sulfur cathodes to improve the discharge capacity and cycling performance of Li-S batteries.^[35]

2.2 Polar host materials

Apart from additives, polar inorganics with special nanostructures have been considered as sulfur hosts to replace the nonpolar carbon matrix. The nanostructured polar inorganics featuring strong polar metal-nonmetal bonding not only can absorb the polysulfides from the point of view of chemical interactions and physical barriers, but also contribute to the volumetric energy density of the Li-S batteries due to their high intrinsic density. Polar nanostructured inorganics used as host materials for Li-S batteries can be divided into three categories, metal oxides, metal sulfides, and MXene materials (metal carbides or carbonitrides) in this section.

2.2.1 Metal oxide hosts

Metal oxides contain oxygen anions in the oxidation state of O²⁻ in polar metal-oxygen bonds, affording abundant polar active sites to absorb the polysulfides. Some typical polar metal oxides (TiO₂, MnO₂, Ti₄O₇) will be discussed in this section to demonstrate the potential of metal oxide hosts for Li-S batteries.

TiO₂ is the most widely investigated polar metal oxide host for Li-S batteries. A sulfur-TiO₂ yolk-shell nanostructured cathode material for Li-S batteries was reported by Cui's group (Figure 1b) in 2013.^[36] Unexpectedly high electrochemical performance could be obtained, and the as-designed sulfur cathode delivered an initial capacity of 1030 mAh g⁻¹ at 0.5 C and capacity decay as small as 0.033% per cycle after 1000 cycles (Figure 1c). This yolk-shell design could supply sufficient space for the volume expansion of sulfur. Although the chemical interaction between the polysulfides and the polar TiO₂ shell was not directly pointed out in this report, the authors claimed that TiO₂ possesses hydrophilic Ti-O groups

and surface hydroxyl groups, which play a decisive role in strongly binding with polysulfides. Many kinds of nanostructured TiO₂, such as hollow spheres,^[37] mesoporous spheres,^[38,39] nanowires,^[40] nanotubes,^[41-43] nanofibers,^[44] nanoparticles,^[45] and feather duster,^[46] were then explored to host sulfur in the cathode.

Nb₂O₅ is an electronic semi-conductor with orthorhombic phase structure, and its bulk electrical conductivity reaches to $3.4 \times 10^{-6} \text{ S cm}^{-1}$.^[47] The Li⁺ intercalation pseudocapacitance behavior of Nb₂O₅ was discovered by Dunn et al.,^[48] as the unique Nb-O crystalline structure could provide fast two-dimensional transport paths for Li⁺ between atomic layers, resulting in the formation of highly conductive lithiated compounds. Tao et al. designed a new effective sulfur host, in which Nb₂O₅ was dispersed into mesoporous carbon microspheres (MCM/Nb₂O₅) through a wet impregnation method (Figure 2a).^[49] With the combination of the high conductivity of the MCM and the high polarity of the Nb₂O₅ nanocrystals, MCM/Nb₂O₅ cathodes delivered an initial discharge capacity of 1289 mAh g⁻¹ at 0.5 C and excellent capacity retention with a fade rate as low as 0.14% per cycle over 200 cycles, as well as good rate capacity of 640 mAh g⁻¹ at 5 C. According to the density functional theory (DFT) calculations, the binding energy between Li₂S₆ and Nb₂O₅ is 65.16 kcal mol⁻¹, while it is only 9.84 kcal between Li₂S₆ and *sp*² carbon (Figure 2b). Figure 2c displays the conformation of the binding system. The shortest distance between Li and O is 0.19 nm, indicating a strong ionic Li-O bond, which mainly accounts for the binding energy between Li₂S₆ and Nb₂O₅. The distance between Nb and S is 0.24-0.27 nm, which also partially improves the interaction between Li₂S₆ and Nb₂O₅ due to the van der Waals attraction and weak ionic bonds. The distance between Li and C is relatively long (0.24 nm), however, resulting in weaker attraction than for the Li-O bond. Additionally, there are four Li-O and four Nb-S pair in the Li₂S₆-Nb₂O₅ system, while there is only one Li-C pair in the Li₂S₆-C system. Furthermore, an electrochemical kinetic study further revealed that the Nb₂O₅ nanocrystals serve as an electrocatalyst, accelerating the multiple polysulfide transformation.

Using MnO_2 as an efficient sulfur host materials was first proposed by Liang et al.^[50] Ultra-thin monoclinic birnessite $\delta\text{-MnO}_2$ nanosheets were synthesized by reducing graphene oxide (GO) with KMnO_4 . In order to demonstrate the ability of the MnO_2 nanosheet host to bind with polysulfides, 75S/ MnO_2 and a control sample, 75S/KB (KB = Ketjen Black) were used to conduct an in-situ visual-electrochemical experiment. Figure 2d clearly shows that the electrolyte in the 75S/KB cell changed from colorless to bright yellow-green on partial discharge of the cell over 4 h. In contrast, the electrolyte for the 75S/ MnO_2 cell exhibited only a faint yellow color at 4 h. This indicates that $\delta\text{-MnO}_2$ nanosheets could effectively trap the polysulfides. In addition, the electrolyte was rendered completely colorless on full discharge, indicating that the MnO_2 nanosheets effectively promoted the conversion from polysulfides to insoluble reduced $\text{Li}_2\text{S}_2/\text{Li}_2\text{S}$. In this special chemical interaction mechanism, the sulfur- MnO_2 nanosheet composite with 75 wt% sulfur displayed an initial capacity of 1300 mA hg^{-1} at C/20 and a fade rate over 2000 cycles of 0.036% per cycle at 2 C. Subsequently, Chen et al. designed a nanocomposite of hollow sulfur spheres decorated by MnO_2 nanosheets, and DFT calculations were further conducted to analyze the binding energy of S_n^{2-} species with MnO_2 during lithiation evolution (Figure 2e).^[51] The binding energies were in the range of -3.86 to -5.15 eV (Figure 2f), which is much higher than the binding energies between S_n^{2-} species and nonpolar carbon materials. This result proves theoretically the strong interaction between MnO_2 and sulfur species. The composite retained a capacity of 1072 mAh g^{-1} after 200 cycles at 0.2 C. Although MnO_2 nanosheets can achieve strong chemical binding of polysulfides, the open structure of itself cannot supply a physical barrier to confine polysulfides. In addition, the insulating properties of MnO_2 still lead to poor rate capability. Therefore, more sophisticated nanostructures of MnO_2 composites combined with highly conductive carbon materials were designed to improve the electrochemical performance of Li-S batteries, including core-shell sulfur- MnO_2 composite,^[52-54] hollow carbon nanofibers filled with MnO_2

nanosheet as host,^[55] polypyrrole-MnO₂ coaxial nanotube host,^[56] and MnO₂@carbon hollow nanoboxes as host^[57]

Realizing the drawback from the highly insulating nature of these metal oxides mentioned above, the nanostructured Magnéli phase oxide Ti₄O₇ was further developed as a polar host for Li-S batteries, because it combines metallic conductivity with strong chemical binding ability towards polysulfides. Ti₄O₇ contains polar O-Ti-O units that have a high affinity for polysulfide, and the theoretical bulk conductivity is as high as $2 \times 10^3 \text{ S cm}^{-1}$ at 298 K. Pang et al. visually tested the interaction between Ti₄O₇ and Li₂S₄.^[58] The Li₂S₄ solvent with the addition of Ti₄O₇ became light yellow immediately and almost completely colorless after 1 h, while the control samples (graphite and carbon in equivalent amounts based on surface area) remained intensely yellow-gold (Figure 3a), indicating a strong interaction between Li₂S₄ and polar Ti₄O₇. The potential mechanism of the chemical interaction was explored by analyzing S 2p X-ray photoelectron spectroscopy (XPS) spectra (Figure 3b). The S_T⁻¹ and S_B⁰ peaks, corresponding to the terminal and bridging sulfur atoms, are shifted to higher energies by 2.7 and 1.7 eV upon contact between Li₂S₄ and Ti₄O₇. This indicates interaction of both the terminal and bridging sulfur in the lithium polysulfides with the Ti₄O₇ surface, resulting in the polarization of electrons away from the sulfur atoms by the electropositive titanium and/or oxygen vacancies at the interface. In addition, the electron transfer to chemically bonded lithium polysulfides is enhanced on the metallic surface of Ti₄O₇, leading to surface-mediated deposition of the discharge product Li₂S. This was evidenced by an operando X-ray absorption near-edge spectroscopy (XANES) study on the Ti₄O₇/S electrode (Figure 3c). At almost the same time, Tao et al. also investigated the Ti₄O₇ materials as host materials in Li-S batteries.^[59] The DFT calculation results for the bonding properties of S_x (x = 1, 2, and 4) and Li₂S_x (x = 1, 2, and 4) on Ti₄O₇ (1-20) and TiO₂ (110) is shown in Figure 3d, which indicates that the low coordinated Ti in titanium oxide can stabilize the sulfur clusters, while oxygen-

rich titanium oxide can stabilize metal clusters because of the formation of strong chemical bonding.

Additionally, many other polar metal oxide composites have been used as sulfur hosts to anchor the polysulfides, such as Fe_3O_4 , CeO_2 , NiFe_2O_4 , Si/SiO_2 , Co_3O_4 , V_2O_5 , and MoO_2 , which significantly improves the electrochemical performance of the Li-S batteries.^[60-69] Due to the intrinsic highly insulating property of metal oxides, the high internal resistance may lead to sluggish interface redox reaction kinetics, decreasing the sulfur utilization and rate capability. Therefore, most polar metal oxide hosts used in the cathode are coupled with conductive polymers or carbon materials to improve the overall conductivity to obtain the best performance. On the other hand, complicated nanostructured polar metal oxide hosts are generally needed in order to obtain abundant interfaces and tunable exposed surfaces.

2.2.2 *Metal sulfide hosts*

Metal sulfides are another class of typical polar inorganics that can accommodate sulfur and anchor polysulfides in Li-S batteries. The conductivity of the metal sulfides is much higher than that of the metal oxides, and some metal sulfides even have metallic or half-metallic phases. As a result, many types of metal sulfides with high conductivity have been explored for Li-S batteries. In this section, the advances in the use of typical polar sulfides as host materials for Li-S batteries are summarized.

The conductivity of pyrite-type CoS_2 crystal is as high as $6.7 \times 10^3 \text{ S cm}^{-1}$ at 300 K. The half-metallic CoS_2 was introduced into graphene/sulfur cathode by Yuan et al.^[70] The binding energy of CoS_2 and Li_2S_4 was found to be as high as 1.97 eV (0.34 eV for graphene) based on the DFT calculation results (Figure 4a), demonstrating the strong interaction between CoS_2 and polysulfides. The interfaces between CoS_2 and the electrolyte also provide strong adsorption and activation sites for polar polysulfides, accelerating the redox reactions of polysulfides. Effective polarization mitigation and enhanced energy efficiency could be guaranteed due to the high reactivity of the polysulfide. The graphene/ CoS_2 composite

containing 75wt % sulfur exhibited a high initial capacity of 1368 mAh g⁻¹ at 0.5 C and a small capacity decay rate of 0.034% per cycle at 2.0 C. The existence of CoS₂ not only anchored the polar polysulfides, but also accelerated the charge transfer at the polysulfide/CoS₂ interface, as illustrated in Figure 4b, enhancing the electrochemical performance of Li-S batteries.

Co₉S₈ is another kind of metal sulfide with high conductivity of 290 S cm⁻¹ at room temperature. Unique Co₉S₈-inlaid carbon hollow nanopolyhedra were synthesized and then used as an efficient sulfur host for Li-S batteries by Chen et al., as shown in Figure 4c.^[71] These hollow nanopolyhedra with large void space not only accommodate high sulfur mass loading, but also buffer the volume expansion. The highly polar embedded Co₉S₈ crystals can strongly bind polysulfides and therefore restrict their outward diffusion. In order to probe the chemisorption capability of Co₉S₈ nanocrystals towards polysulfides, DFT calculations were conducted, as shown in Figure 4d. The (202) planes of Co₉S₈ were chosen as the representative crystalline planes for the simulations, because they are close to the stoichiometric Co/S ratio of 5:4. The absorption energies between Co₉S₈ (202) and the different Li₂S_n species (Li₂S₈, Li₂S₆, Li₂S₄, Li₂S₂, Li₂S) are -6.08, -4.03, -2.97, -4.52, and -5.51 eV, respectively. This strong chemical interaction of Li₂S_n with Co₉S₈ resulted from their highly polar nature. A visual adsorption experiment was further carried out, as shown in Figure 4e. The color of a Li₂S₄ solution mixed with Co₉S₈/C hollow nanocrystals turned almost colorless after 120 min, confirming that the Co₉S₈/C hollow nanocrystals had stronger adsorption capability towards Li₂S₄ than common porous carbon. The Co₉S₈/C-S composite cathode still exhibited high discharge capacity of 560 mAh g⁻¹ after 1000 cycles at 2.0 C, corresponding to a low capacity decay of 0.041% per cycle. In addition, the improved rate performance indicates that Co₉S₈ can also significantly improve the reaction kinetics of the polysulfide redox reactions.

TiS₂ also has been studied in Li-S batteries due to its high electronic conductivity and the polar nature of its surface. Cui and co-workers proposed a Li₂S@TiS₂ core-shell nanostructure synthesized by an in-situ reaction method as cathode for Li-S batteries (Figure 5a).^[72] The TiCl₄ precursor reacts directly with some of the Li₂S on the surface to form a TiS₂ coating (TiCl₄ + 2Li₂S = TiS₂ + 4LiCl), resulting in the formation of the Li₂S@TiS₂ core-shell nanostructure. On the one hand, the electronic conductivity of the Li₂S@TiS₂ structures was measured to be $5.1 \times 10^{-3} \text{ S cm}^{-1}$, which is 10 orders of magnitude higher than that of bare Li₂S ($10^{-3} \text{ S cm}^{-1}$), leading to fast electron transport. On the other hand, polar Ti-S groups in the TiS₂ coating layer can potentially interact strongly with Li₂S_n species, as evidenced by the DFT calculations (Figure 5b). The binding energy between Li₂S and a single layer of TiS₂ was 2.99 eV, while only 0.29 eV was calculated between Li₂S and a single layer of carbon-based graphene.^[73] The much stronger interaction between Li₂S and TiS₂ is attributed to their similar polar nature, unlike the nonpolar nature of graphene. In addition, this similar reaction mechanism can be extended to the synthesis of Li₂S@ZrS₂ and Li₂S@VS₂ core-shell nanostructures. The calculated binding energies of Li₂S to ZrS₂ and VS₂ are 2.70 and 2.94 eV, respectively (Figure 5b). Compared to the bare Li₂S cathodes, the Li₂S@TiS₂ cathodes exhibited a high initial specific capacity of 806 mAh g⁻¹, which was calculated based on Li₂S, stable cycling performance at 0.2 C, and good rate capability from 0.2 to 4 C (Figure 5c). Another study of TiS₂ foam supported sulfur cathode with high sulfur loading was conducted by Archer and co-workers.^[74] The improved performance of the materials was also attributed to the high conductivity and strong affinity towards soluble polysulfides of polar TiS₂.

Various other metal sulfides, such as MoS₂,^[75,76] SnS₂,^[77,78] NiS₂,^[79] WS₂,^[80] MnS,^[81] CuS,^[82] and FeS₂,^[83] have also been investigated as polar hosts in Li-S batteries. Although the conductivity of the metal sulfides is much higher than for metal oxides, carbon-based materials are still introduced, in order to further decrease the internal resistance and enhance the utilization of the active material. In addition, most of the adsorption mechanisms between

metal sulfides and polysulfides are not completely clearly yet and need to be deeply investigated.

2.2.3 *MXene phase material Hosts*

The MXene phase is a family of transition metal carbides or carbonitrides that was first reported by Gogotsi's group,^[84] which are well known for high conductivity in the core and abundant functional groups on the surface. The MXenes are produced by selectively etching A atoms from layered MAX phases ($M_{n+1}AX_n$, where M is transition metal, A is one of a group of IIIA/IVA elements, and X is C or N), and then delaminating the sheets in polar solvent. The delaminated 2D MXene phases possess high conductivity and abundant functional groups on the surface.

Several Ti_xC_y -type MXenes have been explored as sulfur hosts for Li-S batteries. Ti_2C was first reported to be a highly effective cathode host material by Liang et al,^[85] which was prepared by corroding Al atoms from Ti_2AlC . It was found that the unoccupied orbitals of Ti atoms in the surfaces of Ti_2C nanosheets were bound with either -OH or sulfides after exfoliation and delamination treatment (Figure 6a). Although Ti_2C nanosheet has neither porous structure nor high specific surface area, unexpectedly superior properties still were obtained when it was employed as a sulfur host material. This indicates that the chemical bonding with polysulfides effectively suppressed the dissolution and diffusion of the polysulfides, which is supported by XPS analysis (Figure 6b). The Ti 2p XPS spectrum of 70S/ Ti_2C sample exhibited an additional peak at 457.6 eV assigned to the S-Ti-C bonds, which is also found in Li_2S_4 - Ti_2C and fully discharged 70S/ Ti_2C electrode. This implies that the -OH functional groups were substituted by sulfur species. Therefore, the analysis mentioned above proves that there exists a strong chemical interaction between the polysulfides and the nanosheets, enhancing the electrochemical stability of the Ti_2C/S composite. After that, Liang et al. further investigated the MXene phases Ti_3C_2 and Ti_3CN as sulfur hosts, with XPS and DFT calculations results also demonstrating the strong interaction

between polysulfides and MXene phase Ti_3C_2 .^[86] Recently, Zhang et al. investigated the crucial role of the conductivity of the polar host in the electrochemical kinetics of Li-S batteries by using conductive TiC as sulfur host.^[87] The interfacial electrochemical kinetics are determined by two main factors, illustrated in Figure 6c, which include adequate binding affinity and efficient charge transfer over the liquid-solid boundary during the redox reactions of the adsorbates. As a nonpolar host, carbon is too inert to bind polar polysulfides, leading to low coverage of reactive intermediates. A polar insulator such as TiO_2 possesses a strong affinity towards absorbing the polysulfides on the surface, but its low conductivity hinders direct surface conversion on the polar host. Therefore, only polar materials with high conductivity can fully meet the demands for both sufficient surface binding and efficient charge transport, resulting in enhanced electrochemical kinetics. DFT calculation results showed that the binding energies between TiC (100) and Li_2S_4 and Li_2S are -1.89 eV and -2.75 eV, respectively, which were significantly higher than those on the graphene plane (Figure 6d). Highly conductive TiC was proved to promote the liquid-liquid transformation of polysulfides as well as the liquid-solid nucleation/growth of Li_2S , resulting in enhanced electrochemical performance.

In summary, the polar inorganics, including metal oxides, metal sulfides, and MXene phase materials, have been proved to strongly anchor the polar polysulfides (Table 1). The polar-polar interaction between polar inorganics and polysulfides plays an important role, and nanostructures also contribute to the improved electrochemical performance. Even so, the role of intrinsic properties and correlation with the electrical conductivity for the polar inorganics is not fully understood. Theoretical calculation and prediction may be an effective strategy to guide the future development of polar inorganics for Li-S batteries.

3. Polar organics used in binder for Li-S batteries

Poly(vinylidene difluoride) (PVDF) is the conventional binder that is used in Li-S batteries, although it just provides physical adhesion to link the active materials to the current collector.

Due to its linear molecular structure, there is no bonding between the binder and the polysulfides, leading to the dissolution of polysulfides in the organic electrolyte. Therefore, the design of a polar binder capable of absorbing polar polysulfides would be more desirable to advance the application of Li-S batteries. The study of polar binders for Li-S is at an early stage, and only a few reported polar binders that have been used as multifunctional binders in Li-S batteries are reviewed in this section.

3.1 Amino functional group binder

Polar polyethylenimine (PEI) polymer has been used as the binder in Li-S batteries due to its abundant amino groups and branched structure, which can provide strong affinity to absorb polysulfide.^[88] Recently, another multifunctional amino functional group (AFG) polar binder was reported by Yan et al.^[89] The AFG binder was synthesized by polymerization of hexamethylene diisocyanate (HDI) with PEI polymer in dimethyl formamide (DMF) solvent. The obtained AFG binder possesses a unique chemical structure with abundant polar amine groups and a hyper-branched network (Figure 7a), which can provide strong interaction with polysulfide intermediates. The ^{13}C NMR spectrum of AFG clearly shows the polar amide groups (N-CH=O, N=C-OH, and C-C-NH₂). In addition, the AFG binder exhibits good flexibility and the stretchability can be up to over 70% (Figure 7b). According to the DFT calculation results, the binding energy between AFG binder and Li₂S_n species is significantly higher than the binding energy between Li₂S_n and PVDF binder (Figure 7c).^[90] All these features endow the sulfur cathode with AFG binder with good electrochemical properties. The as-prepared sulfur cathode showed remarkably enhanced cycling performance with capacity retention of 91.3% at 2 C after 600 cycles, which is attributed to the unique polar amine molecule of the binder, absorbing the polar polysulfides to suppress the shuttle effect. On the other hand, the issue of volume expansion could be solved because of the elastic and mechanical properties of the binder. More importantly, the cathode material used in this

experiment is commercial sulfur powder without any special engineered properties, so the new design of the AFG binder can greatly promote the practical application of Li-S batteries.

Jiao et al. synthesized another multi-functional binder (AHP), with abundant amide groups as an efficient binder for Li-S batteries.^[91] The polar AHP binder prepared by polymerization of HDI with ethylenediamine (EDA) contains a large amount of amino groups, which can strongly anchor the polysulfides, thus suppressing the shuttle effect. Figure 7d shows the design concept and a schematic illustration of the synthesis of the polar AHP binder, with a series of polar amide groups introduced into the AHP binder during polymerization. Compared to the commercial binders, the amide polar groups in the novel binder could strongly anchor Li_2S_n species to effectively keep them within the cathode region, improving the electrochemical stability of the Li-S batteries. A schematic illustration of the evolution of AHP and commercial PVDF binder during cycling, as shown in Figure 7e, indicates that the AHP binder not only can tolerate the massive volume change of sulfur cathode during the discharge process, but also maintains the strong interactions between the polysulfides and the binder even during the charge process. All these advantageous features of AHP binder endow the C/S composite (60 wt% S) cathodes with excellent capacity stability.

3.2 Copolymers of vinylidene difluoride (VDF) with different monomers

Our group used copolymers of VDF with other monomers, e.g. poly(vinylidene difluoride-trifluoroethylene) (P(VDF-TRFE)), as binders to improve the electrochemical performance of Li-S batteries.^[92] Figure 8a shows the molecular structure of PVDF and its copolymers with other monomers. From the point of view of chemical structure, there are two fluorine atoms in the monomer unit of PVDF but five fluorine atoms and one hydrogen in P(VDF-TRFE). For P(VDF-co-CTFE), the hydrogen in the trifluoroethylene is replaced by a chloride atom. The modification observed in the monomer unit leads to enhanced molecular polarity of the VDF based copolymers, which have a strong affinity to lithium polysulfides. In addition, the ab-initio simulations performed in the framework of density functional theory clearly confirm the

strong interactions between Li_2S (Li-S species) and the polymer binders (Figure 8b and 8c). The strongest interaction with Li_2S or Li-S species can be observed in the case where it bonds with the -F group in P(VDF-TRFE) binder, with binding energy of 1.05 eV and 0.876 eV, respectively, which is higher than for bonds with PVDF binder. The chemical structure and theoretical calculation results indicate that the -F group in the P(VDF-TRFE) binder possesses a stronger affinity to Li_2S and lithium polysulfides than it does in the PVDF binder, leading to enhanced electrochemical performance. (Figure 8d).

In conclusion, these polar organics used as binder greatly enhanced the electrochemical performance of Li-S batteries (Table 2) because of their inherent functional polar groups, chemically binding the polysulfides. The processing of the new polar organic binders is usually complicated, however, and the cost is relatively high. Apart from strong chemical polysulfide-trapping capability, future polar organic binders should possess other features, low cost and high physical adhesion, to guarantee the high sulfur loading, realizing the practical application of Li-S batteries.

4. Summary and Outlook

In this mini review, we provide an overview of recent advances in the use of polar materials for Li-S batteries. The polar materials discussed here can be divided into two categories, polar inorganics used in the cathode and polar organics used in the binder for Li-S batteries.

On the one hand, the polar inorganics, such as metal oxides, metal sulfides, and MXene phase materials, have been proved to strongly anchor the polar polysulfides from both theoretical and experimental results, suppressing the shuttle effect and prolonging the lifespan of the Li-S batteries. Although the chemical absorption mechanism of these polar inorganics and their impact on the electrochemical kinetics has been partly understood by the traditional characterization methods, e.g. visual absorption test, XPS measurement, and theoretical calculation, some more advanced characterization techniques are further needed to deeply understand it, such as in-situ techniques. In terms of theoretical prediction analysis, apart from

DFT calculation, other new effective theoretical strategies are very much required to give assistance to the selection of suitable sulfur host among thousands of polar inorganics for Li-S batteries. Besides, nanostructure is also an influencing factor on the properties of the polar materials, such as surface area, pore size, and pore volume, affecting the adsorption capability of the polysulfides. For real practical application of Li-S batteries in the near future, general principle for the rational design of nanostructured polar inorganic hosts is strongly required to maintain the balance among the adsorption capability, sulfur loading mass, and product cost. On the other hand, the research on polar organics used in binders for Li-S batteries is in its early stages. There are a few research reports on polar organics as binders, demonstrating their strong interaction with polysulfides. The ability of polar binders to adsorb polysulfides is mainly determined by their intrinsic polarity. Therefore, the quantity and type of the introduced functional polar groups should be taken into account in designing and synthesizing the novel polar binder, enhancing its polarity as much as possible. In addition to guaranteeing the integrity of the whole electrode and uniform distribution of the cathode materials, we believe that functional binders in the future should possess the features of low cost and high physical adhesion, as well as strong chemical polysulfide-trapping capability.

Acknowledgements

This work was supported by the National Natural Science Foundation of China (51702079) and the Australian Research Council (ARC) through an ARC Discovery project (DP170102406) and a Future Fellowship (FT150100109). Furthermore, the authors are grateful to Dr Tania Silver for critical reading of the manuscript.

Received: ((will be filled in by the editorial staff))
Revised: ((will be filled in by the editorial staff))
Published online: ((will be filled in by the editorial staff))

References

- [1] P. G. Bruce, S. A. Freunberger, L. J. Hardwick, J. M. Tarascon, *Nat. Mater.* **2012**, *11*, 19.
- [2] S. E. Cheon, S. S. Choi, J. S. Han, Y. S. Choi, B. H. Jung, H. S. Lim, *J. Electrochem. Soc.* **2004**, *151*, A2067.
- [3] Y. Yang, G. Y. Zheng, S. Misra, J. Nelson, M. F. Toney, Y. Cui, *J. Am. Chem. Soc.* **2012**, *134*, 15387.
- [4] Y. X. Ren, T. S. Zhao, M. Liu, L. Wei, R. H. Zhang, *Electrochim. Acta*, **2017**, *242*, 137.
- [5] X. L. Ji, K. T. Lee, L. F. Nazar, *Nat. Mater.* **2009**, *8*, 500.
- [6] Z. Li, J. T. Zhang, X. W. Lou, *Angew. Chem. Int. Ed.* **2015**, *54*, 12886.
- [7] Y.V. Mikhaylik, J.R. Akridge, *J. Electrochem. Soc.* **2004**, *151*, A1969.
- [8] Y. Yang, G.Y. Zheng, Y. Cui, *Chem. Soc. Rev.* **2013**, *42*, 3018.
- [9] Y. Zhao, M. Liu, W. Lv, Y. B. He, C. Wang, Q. B. Yun, B. H. Liu, F. Y. Kang, Q. H. Yang, *Nano Energy*, **2016**, *30*, 1.
- [10] G. M. Liang, J. X. Wu, X. Y. Qin, M. Liu, Q. Li, Y. B. He, J. K. Kim, B. H. Li, F. Y. Kang, *ACS Appl. Mater. Interfaces*, **2016**, *8*, 23105.
- [11] N. Jayaprakash, J. Shen, S. S. Moganty, A. Corona, L. A. Archer, *Angew. Chem. Int. Ed.* **2011**, *50*, 5904.

- [12] C. F. Zhang, H. B. Wu, C. Yuan, Z. P. Guo, X. W. Lou, *Angew. Chem. Int. Ed.* **2012**, *51*, 9592.
- [13] S. Y. Zheng, Y. Chen, Y. H. Xu, F. Yi, Y. J. Zhu, Y. H. Liu, J. H. Yang, C. S. Wang, *ACS Nano* **2013**, *7*, 10995.
- [14] C. D. Liang, N. J. Dudney, J. Y. Howe, *Chem. Mater.* **2009**, *21*, 4724.
- [15] L. W. Ji, M. M. Rao, S. Aloni, L. Wang, E.J. Cairns, Y. G. Zhang, *Energy Environ. Sci.* **2011**, *4*, 5053.
- [16] Z. Li, Y. Jiang, L. X. Yuan, Z. Q. Yi, C. Wu, Y. Liu, P. Strasser, Y. H. Huang, *ACS Nano* **2014**, *8*, 9295.
- [17] Z. Yuan, H. J. Peng, J. Q. Huang, X. Y. Liu, D. W. Wang, X. B. Cheng, Q. Zhang, *Adv. Funct. Mater.* **2014**, *24*, 6105.
- [18] H. Q. Wang, C. F. Zhang, Z. X. Chen, H. K. Liu, Z. P. Guo, *Carbon* **2015**, *81*, 782.
- [19] Y. Zhao, W. L. Wu, J. X. Li, Z. C. Xu, L. H. Guan, *Adv. Mater.* **2014**, *26*, 5113.
- [20] D. S. Jung, T. H. Hwang, J. H. Lee, H. Y. Koo, R. A. Shakoob, R. Kahraman, Y. N. Jo, M. S. Park, J. W. Choi, *Nano Lett.* **2014**, *14*, 4418.
- [21] L. W. Ji, M. M. Rao, H. M. Zheng, L. Zhang, Y. C. Li, W. H. Duan, J. H. Guo, E. J. Cairns, Y. G. Zhang, *J. Am. Chem. Soc.* **2011**, *133*, 18522.

- [22] M. Q. Zhao, Q. Zhang, J. Q. Huang, G. L. Tian, H. J. Peng, F. Wei, *Nat. Commun.* **2014**, 5, 3410.
- [23] C. X. Zu, A. Manthiram, *Adv. Energy Mater.* **2013**, 3, 1008.
- [24] J. X. Song, M. L. Gordin, T. Xu, S. R. Chen, Z. X. Yu, H. Sohn, J. Lu, Y. Ren, Y. H. Duan, D. H. Wang, *Angew. Chem. Int. Ed.* **2015**, 54, 4325.
- [25] G. M. Zhou, L. C. Yin, D. W. Wang, L. Li, S. F. Pei, I. R. Gentle, F. Li, H. M. Cheng, *ACS Nano* **2013**, 7, 5367.
- [26] C. P. Yang, Y. X. Yin, H. Ye, K. C. Jiang, J. Zhang, Y. G. Guo, *ACS Appl. Mater. Interfaces* **2014**, 6, 8789.
- [27] Q. Pang, J. T. Tang, H. Huang, X. Liang, C. Hart, K.C. Tam, L.F. Nazar, *Adv. Mater.* **2015**, 27, 6021.
- [28] Y. L. Ding, P. Kopold, K. Hahn, P. A. van Aken, J. Maier, Y. Yu, *Adv. Funct. Mater.* **2016**, 26, 1112.
- [29] M. S. Song, S. C. Han, H. S. Kim, J. H. Kim, K. T. Kim, Y. M. Kang, H. J. Ahn, S. X. Dou, J. J. Lee, *J. Electrochem. Soc.* **2004**, 151, A791.
- [30] Y. J. Choi, B. S. Jung, D. J. Lee, J. H. Jeong, K. W. Kim, H. J. Ahn, K. K. Cho, H. B. Gu, *Phys. Scripta* **2007**, 129, 62.

- [31] G. Zhou, E. Paek, G.S. Hwang, A. Manthiram, *Nat. Commun.* **2015**, 6, 7760.
- [32] X. Gu, C. Tong, C. Lai, J. Qiu, X. Huang, W. Yang, B. Wen, L. Liu, Y. Hou, S. Zhang, *J. Mater. Chem. A* **2015**, 3, 16670.
- [33] W. Zheng, X. Hu, C. Zhang, *Electrochem. Solid State Lett.* **2006**, 9, A364.
- [34] S. Evers, T. Yim, L. F. Nazar, *J. Phys. Chem. C* **2012**, 116, 19653.
- [35] X. L. Ji, S. Evers, R. Black, L. F. Nazar, *Nat. Commun.* **2011**, 2, 325.
- [36] Z. W. Seh, W. Y. Li, J. J. Cha, G. Y. Zheng, Y. Yang, M. T. McDowell, *Nat. Commun.* **2013**, 4, 1331.
- [37] A. Le Viet, M. V. Reddy, R. Jose, B. V. R. Chowdari, S. Ramakrishna, *J. Phys. Chem. C* **2010**, 114, 664.
- [38] J. W. Kim, V. Augustyn, B. Dunn, *Adv. Energy Mater.* **2011**, 2, 141.
- [39] Y. Q. Tao, Y. J. Wei, Y. Liu, J. T. Wang, W. M. Qiao, L. C. Ling, D. H. Long, *Energy Environ. Sci.* **2016**, 9, 3230.
- [40] H. N. Fan, Q. L. Tang, X. H. Chen, B. B. Fan, S. L. Chen, A. P. Hu, *Chem. Asian J.* **2016**, 11, 2911.
- [41] C. Z. Yuan, S. Q. Zhu, H. Cao, L. R. Hou, J. D. Lin, *Nanotechnology* **2016**, 27, 045403.

- [42] J. Y. Hwang, H. M. Kim, S. K. Lee, J. H. Lee, A. Abouimrane, M. A. Khaleel, I. Belharouak, A. Manthiram, Y. K. Sun, *Adv. Energy Mater.* **2016**, *6*, 1501480.
- [43] Y. C. Yan, T. Y. Lei, Y. Jiao, C. Y. Wu, J. Xiong, *Electrochim. Acta* **2018**, *264*, 20.
- [44] X. Y. Qian, X. L. Yang, L. Jin, D. W. Rao, S. S. Yao, X. Q. Shen, K. S. Xiao, S. B. Qin, J. Xiang, *Mater. Res. Bull.* **2017**, *95*, 402. [t](#)
- [45] Y. Zhao, W. Zhu, G. Z. Chen, E. J. Cairns, *J. Power Sources* **2016**, *327*, 447.
- [46] J. H. Song, J. M. Zheng, S. Feng, C. Z. Zhu, S. F. Fu, W. G. Zhao, D. Du, Y. H. Lin, *Carbon* **2018**, *128*, 63.
- [47] X. Z. Ma, B. Jin, H. Y. Wang, J. Z. Hou, X. Bin Zhong, H. H. Wang, P. M. Xin, *J. Electroanal. Chem.* **2015**, *736*, 127.
- [48] Y. Y. Li, Q. F. Cai, L. Wang, Q. W. Li, X. Peng, B. Gao, K. F. Huo, P. K. Chu, *ACS Appl. Mater. Interfaces* **2016**, *8*, 23784.
- [49] T. Y. Lei, Y. M. Xie, X. F. Wang, S. Y. Miao, J. Xiong, C. L. Yan, *Small* **2017**, *13*, 1701013.
- [50] X. Liang, C. Hart, Q. Pang, A. Garsuch, T. Weiss, L. F. Nazar, *Nat. Commun.* **2015**, *6*, 5682.

- [51] X. L. Wang, G. Li, J. D. Li, Y. N. Zhang, A. Wook, A. P. Yu, Z. W. Chen, *Energy Environ. Sci.* **2016**, *9*, 2533.
- [52] X. Liang, L. F. Nazar, *ACS Nano*, **2016**, *10*, 4192.
- [53] L. B. Ni, Z. Wu, G. J. Zhao, C. Y. Sun, C. Q. Zhou, X. X. Gong, G. W. Diao, *Small*, **2017**, *13*, 1603466.
- [54] S. A. Ahad, P. Ragupathy, S. Ryu, H. W. Lee, D. K. Kim, *Chem. Commun.* **2017**, *53*, 8782.
- [55] Z. Li, J. T. Zhang, X. W. Lou, *Angew. Chem. Int. Ed.* **2015**, *54*, 12886.
- [56] J. Zhang, Y. Shi, Y. Ding, W. K. Zhang, G. H. Yu, *Nano Lett.* **2016**, *16*, 7276.
- [57] S. Rehman, T. Y. Tang, Z. Ali, X. X. Huang, Y. L. Hou, *Small*, **2017**, *13*, 1700087.
- [58] Q. Pang, D. Kundu, M. Cuisinier, L. F. Nazar, *Nat. Commun.* **2014**, *5*, 4759.
- [59] X. Y. Tao, J. G. Wang, Z. G. Ying, Q. X. Cai, G. Y. Zheng, Y. P. Gan, H. Huang, Y. Xia, C. Liang, W. K. Zhang, Y. Cui, *Nano Lett.* **2014**, *14*, 5288.
- [60] J. R. He, L. Luo, Y. F. Chen, A. Manthiram, *Adv. Mater.* **2017**, *29*, 1702707.
- [61] L. B. Ma, R. P. Chen, G. Y. Zhu, Y. Hu, Y. R. Wang, T. Chen, J. Liu, Z. Jin, *ACS Nano*, **2017**, *11*, 7274.

- [62] G. Q. Ma, Z. Y. Wen, Q. S. Wang, J. Jin, X. W. Wu, J. C. Zhang, *J. Inorg. Mater.* **2015**, *30*, 913.
- [63] H. Q. Wang, T. F. Zhou, D. Li, H. Gao, G. P. Gao, A. J. Du, H. K. Liu, Z. P. Guo, *ACS Appl. Mater. Interfaces* **2017**, *9*, 4320.
- [64] Q. Fan, W. Liu, Z. Weng, Y. M. Sun, H. L. Wang, *J. Am. Chem. Soc.* **2015**, *137*, 12946.
- [65] S. Rehman, S. J. Guo, Y. L. Hou, *Adv. Mater.* **2016**, *28*, 3167.
- [66] Z. Chang, H. Dou, B. Ding, J. Wang, Y. Wang, X. D. Hao, D. R. Mac Farlane, *J. Mater. Chem. A* **2017**, *5*, 250.
- [67] W. Li, J. Hicks-Garner, J. Wang, J. Liu, A. F. Gross, E. Sherman, J. Graetz, J. J. Vajo, P. Liu, *Chem. Mater.* **2014**, *26*, 3403.
- [68] M. Liu, Q. Li, X. Y. Qin, G. M. Liang, W. J. Han, D. Zhou, Y. B. He, B. H. Li, F. Y. Kang, *Small* **2017**, *13*, 1602539.
- [69] Q. T. Qu, T. Gao, H. Y. Zheng, Y. Wang, X. Y. Li, X. X. Li, J. M. Chen, J. Shao, H. H. Zheng, *Adv. Mater. Interfaces* **2015**, *2*, 1500048.
- [70] Z. Yuan, H. J. Peng, T. Z. Hou, J. Q. Huang, C. M. Chen, D. W. Wang, X. B. Cheng, F. Wei, Q. Zhang, *Nano Lett.* **2016**, *16*, 519.

[71] T. Chen, L. B. Ma, B. R. Cheng, R. P. Chen, Y. Hu, G. Y. Zhu, Y. R. Wang, J. Liang, Z.

X. Tie, J. Liu, Z. Jin, *Nano Energy* **2017**, *38*, 239.

[72] Z. W. Seh, J. H. Yu, W. Y. Li, P. C. Hsu, H. T. Wang, Y. M. Sun, H. B. Yao, Q. F.

Zhang, Y. Cui, *Nat. Commun.* **2014**, *5*, 5017.

[73] G. Y. Zheng, Q. F. Zhang, J. J. Cha, Y. Yang, W. Y. Li, Z. W. She, Y. Cui, *Nano Lett.*

2013, *13*, 1265.

[74] L. Ma, S. Y. Wei, H. L. L. Zhuang, K. E. Hendrickson, R. G. Hennig, L. A. Archer, *J.*

Mater. Chem. A, **2015**, *3*, 19857.

[75] H. Wang, Q. Zhang, H. Yao, Z. Liang, H.W. Lee, P.C. Hsu, G. Zheng, Y. Cui, *Nano Lett.*

2014, *14*, 7138.

[76] Z. T. Li, S. Z. Deng, R. F. Xu, L. Q. Wei, X. Su, M. B. Wu, *Electrochim. Acta* **2017**, *252*,

200.

[77] X. N. Li, Y. Lu, Z. G. Hou, W. Q. Zhang, Y. C. Zhu, Y. T. Qian, J. W. Liang, Y. T. Qian,

ACS Appl. Mater. Interfaces **2016**, *8*, 19550.

[78] X. L. Li, L. B. Chu, Y. Y. Wang, L. S. Pan, *Mater. Sci. Eng. B* **2016**, *205*, 46.

[79] Y. Lu, X. N. Li, J. W. Liang, L. Hu, Y. C. Hu, Y. T. Qian, *Nanoscale* **2016**, *8*, 17616.

- [80] T. Y. Lei, W. Chen, J. W. Huang, C. Y. Yan, H. X. Sun, C. Wang, W. L. Zhang, Y.R. Li, J. Xiong, *Adv. Energy Mater.* **2017**, *7*, 1601843.
- [81] J. D. Liu, X. S. Zheng, Z. F. Shi, S. Q. Zhang, *Ionics*, **2013**, *20*, 659.
- [82] K. Sun, D. Su, Q. Zhang, D. C. Bock, A. C. Marschlok, K. J. Takeuchi, E. S. Takeuchi, H. Gan, *J. Electrochem. Soc.* **2015**, *162*, A2834.
- [83] S. S. Zhang, D.T. Tran, *J. Mater. Chem. A* **2016**, *4*, 4371.
- [84] M. Naguib, M. Kurtoglu, V. Presser, J. Lu, J. J. Niu, M. Heon, L. Hultman, Y. Gogotsi, M.W. Barsoum, *Adv. Mater.* **2011**, *23*, 4248.
- [85] X. Liang, A. Garsuch, L. F. Nazar, *Angew. Chem. Int. Ed.* **2015**, *54*, 3907.
- [86] X. Liang, Y. Rangom, C. Y. Kwok, Q. Pang, L. F. Nazar, *Adv. Mater.* **2017**, *29*, 1603040.
- [87] H. J. Peng, G. Zhang, X. Chen, Z. W. Zhang, W. T. Xu, J. Q. Huang, Q. Zhang, *Angew. Chem. Int. Ed.* **2016**, *55*, 12990.
- [88] L. Zhang, M. Ling, J. Feng, G. Liu, J. H. Guo, *Nano Energy* **2017**, *40*, 559.
- [89] W. Chen, T. Qian, J. Xiong, N. Xu, X. J. Liu, J. Liu, J. Q. Zhou, X. W. Shen, T. Z. Yang, Y. Chen, C. L. Yan, *Adv. Mater.* **2017**, *29*, 1605160.
- [90] W. S. Zhi, Q. Zhang, W. Li, G. Zheng, H. Yao, Y. Cui, *Chem. Sci.* **2013**, *4*, 3673.

[91] Y. Jiao, W. Chen, T. Y. Lei, L. P. Dai, B. Chen, C. Y. Wu, J. Xiong, *Nanoscale Res. Lett.*

2017, *12*, 195.

[92] H. Q. Wang, V. Sencadas, G. P. Gao, H. Gao, A. J. Du, H. K. Liu, Z. P. Guo, *Nano*

Energy **2016**, *26*, 722.

[93] H. Gao, Q. Lu, Y. J. Yao, X. H. Wang, F. S. Wang, *Electrochim. Acta* **2017**, *232*, 414.

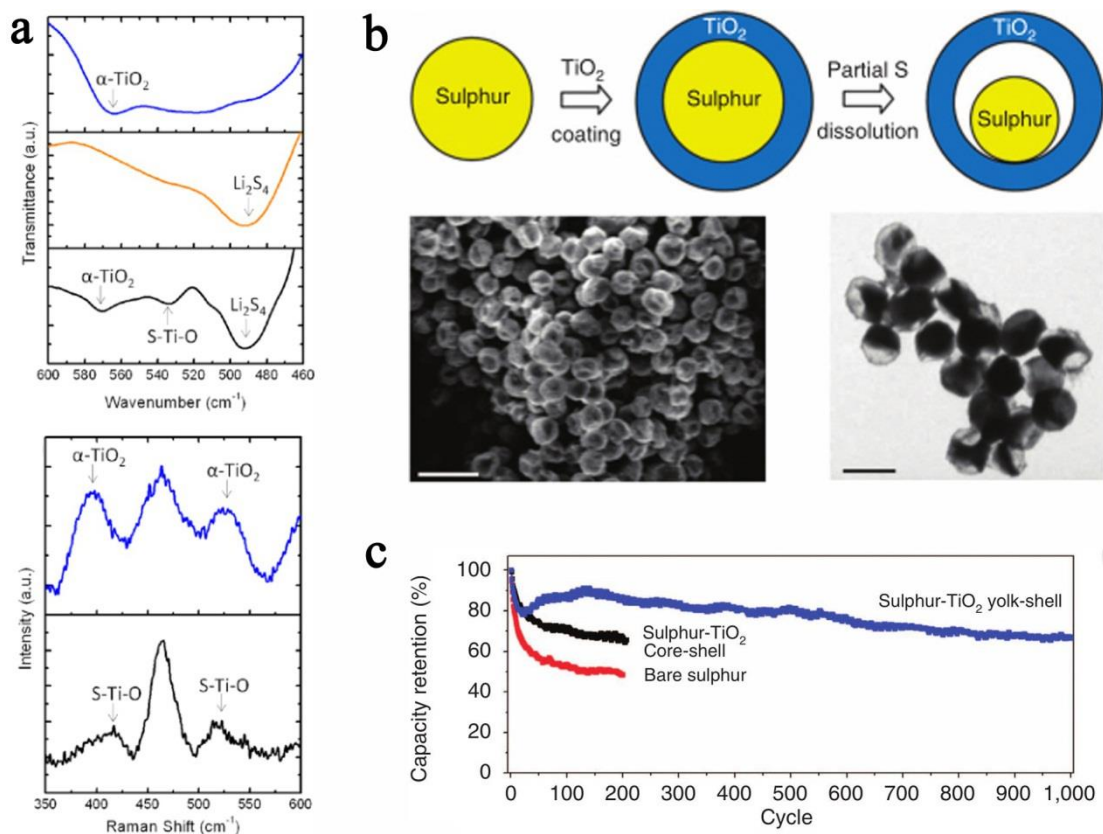


Figure 1. The use of TiO₂ for Li-S batteries. a) FTIR spectra (top) of α -TiO₂, Li₂S₄, and α -TiO₂/Li₂S₄, and Raman spectra (bottom) of α -TiO₂ and α -TiO₂/Li₂S₄. Peaks characteristic of the material are highlighted with arrows. b) Schematic diagram of the synthetic process (top), and SEM and TEM images (bottom) of as-synthesized sulfur-TiO₂ yolk-shell nanostructures. Scale bars, 2 μ m and 1 μ m for SEM and TEM, respectively. c) Capacity retention of sulfur-TiO₂ yolk-shell nanostructures and control samples cycled at 0.5 C. a) Reproduced with permission.^[34] Copyright 2012, American Chemical Society. b,c) Reproduced with permission.^[36] Copyright 2013, Nature Publishing Group.

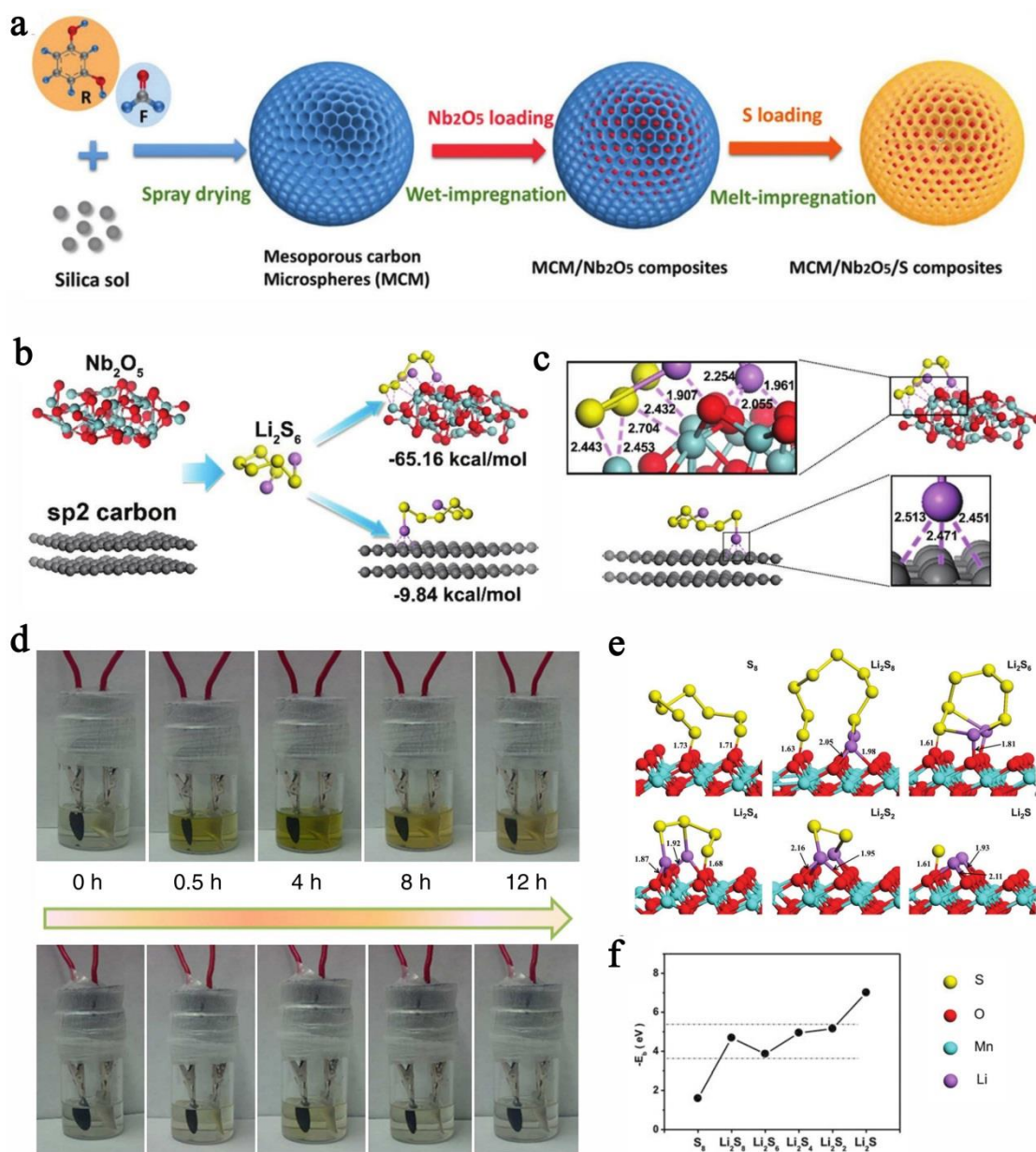


Figure 2. a) Schematic illustration of the synthesis process of the MCM/Nb₂O₅/S composite. b) Binding geometric configurations and energies of a Li₂S₆ molecule with two-layer graphene and Nb₂O₅, which is derived from ab initio calculations based on DFT. c) Conformation of the binding system. d) Visual confirmation of polysulfide entrapment at specific discharge depths (75S/KB, top; and 75S/MnO₂, bottom). e) Optimized configurations for the binding of S, polysulfides, and Li₂S to the MnO₂. f) The binding energies of lithium polysulfides at six different lithiation stages with MnO₂. a-c) Reproduced with permission.^[49] Copyright 2016, Royal Society of Chemistry. d) Reproduced with permission.^[50] Copyright 2015, Nature Publishing Group. e,f) Reproduced with permission.^[51] Copyright 2016, Royal Society of Chemistry.

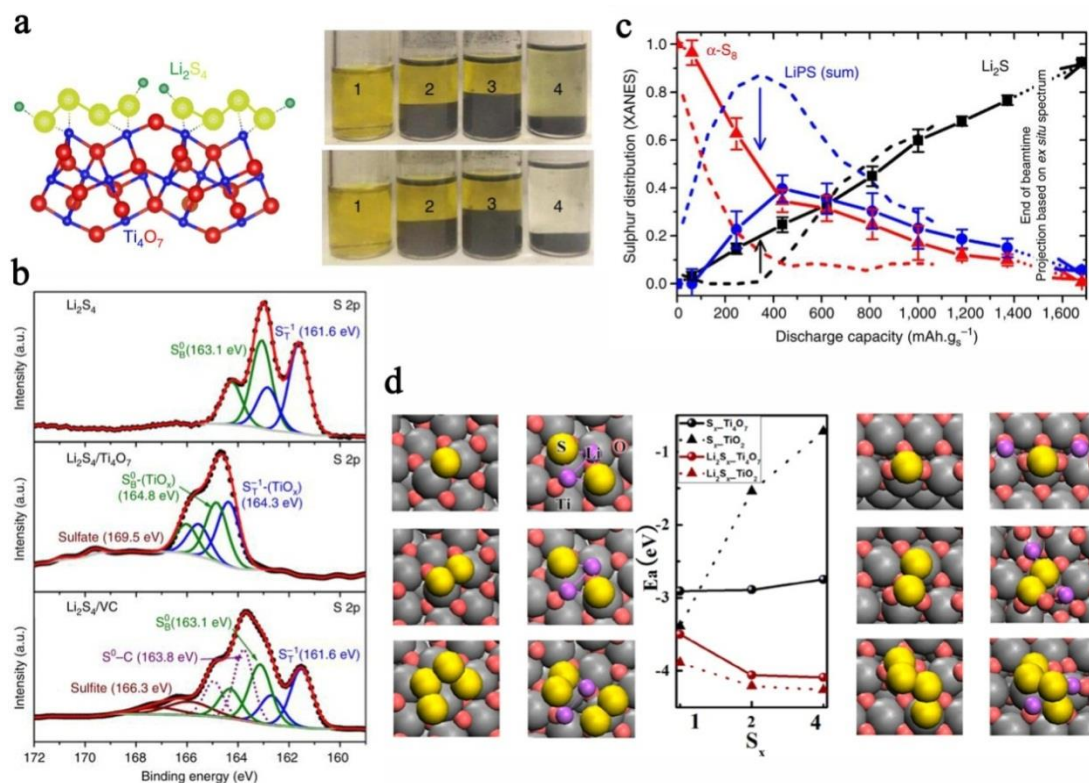


Figure 3. a) Schematic diagram showing the electron density transfer between Li_2S_4 and TiO_x (yellow: S, green: Li, blue: Ti, red: O) (left) and vials of a Li_2S_4 /tetrahydrofuran (THF) solution (1), and the same solution immediately upon contact (top) and after 1 h stirring contact (bottom) with graphite (2), VULCAN XC72 carbon (VC) (3), and Ti_4O_7 (4) (right). b) High-resolution XPS S 2p spectra of Li_2S_4 , $\text{Li}_2\text{S}_4/\text{Ti}_4\text{O}_7$, and $\text{Li}_2\text{S}_4/\text{VC}$. c) Distribution of sulfur species for $\text{Ti}_4\text{O}_7/\text{S-60}$ and VC carbon/S-60 cathodes upon discharge, as determined by operando XANES. d) DFT analysis of the adsorption of S species on Ti_4O_7 (1-20) and TiO_2 (110) surfaces. a-c) Reproduced with permission.^[58] Copyright 2014, Nature Publishing Group. d) Reproduced with permission.^[59] Copyright 2014, American Chemical Society.

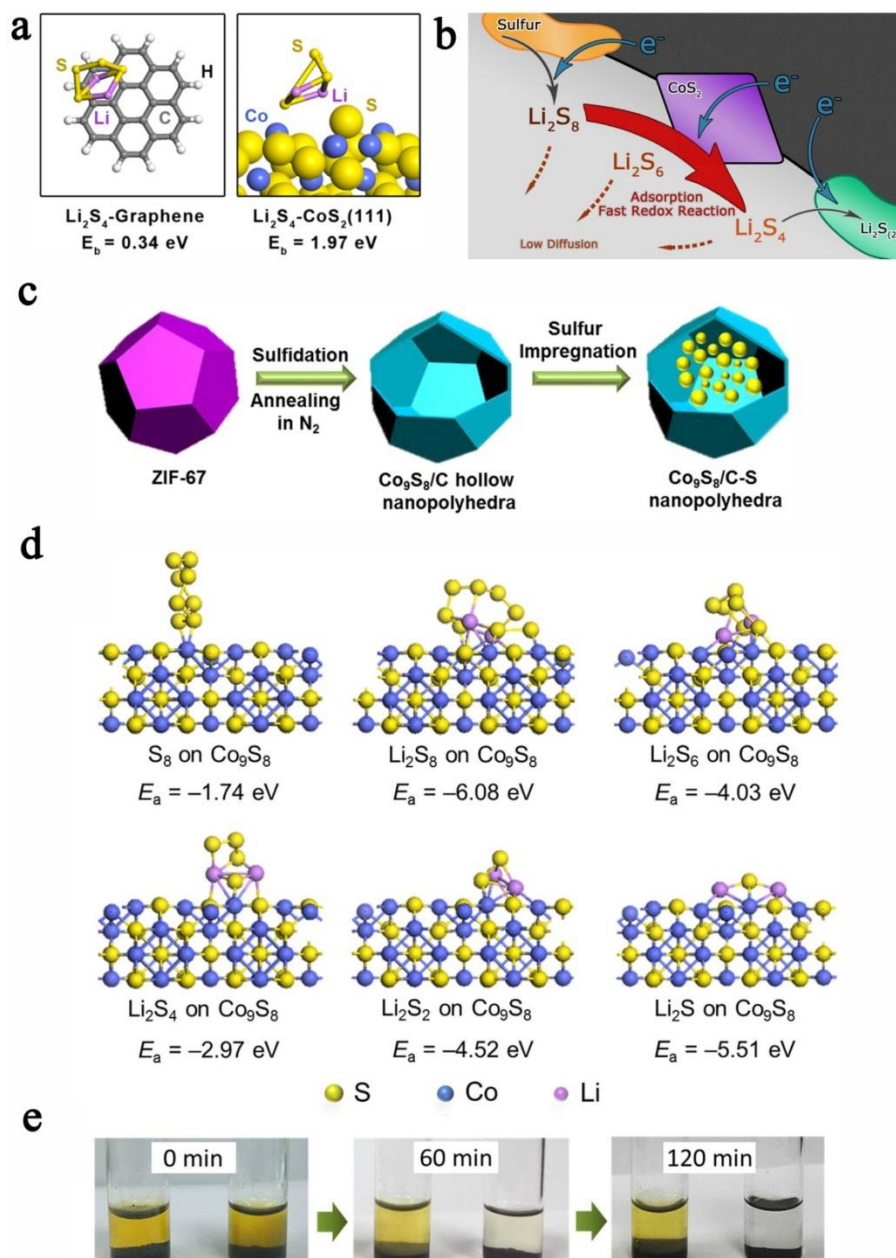
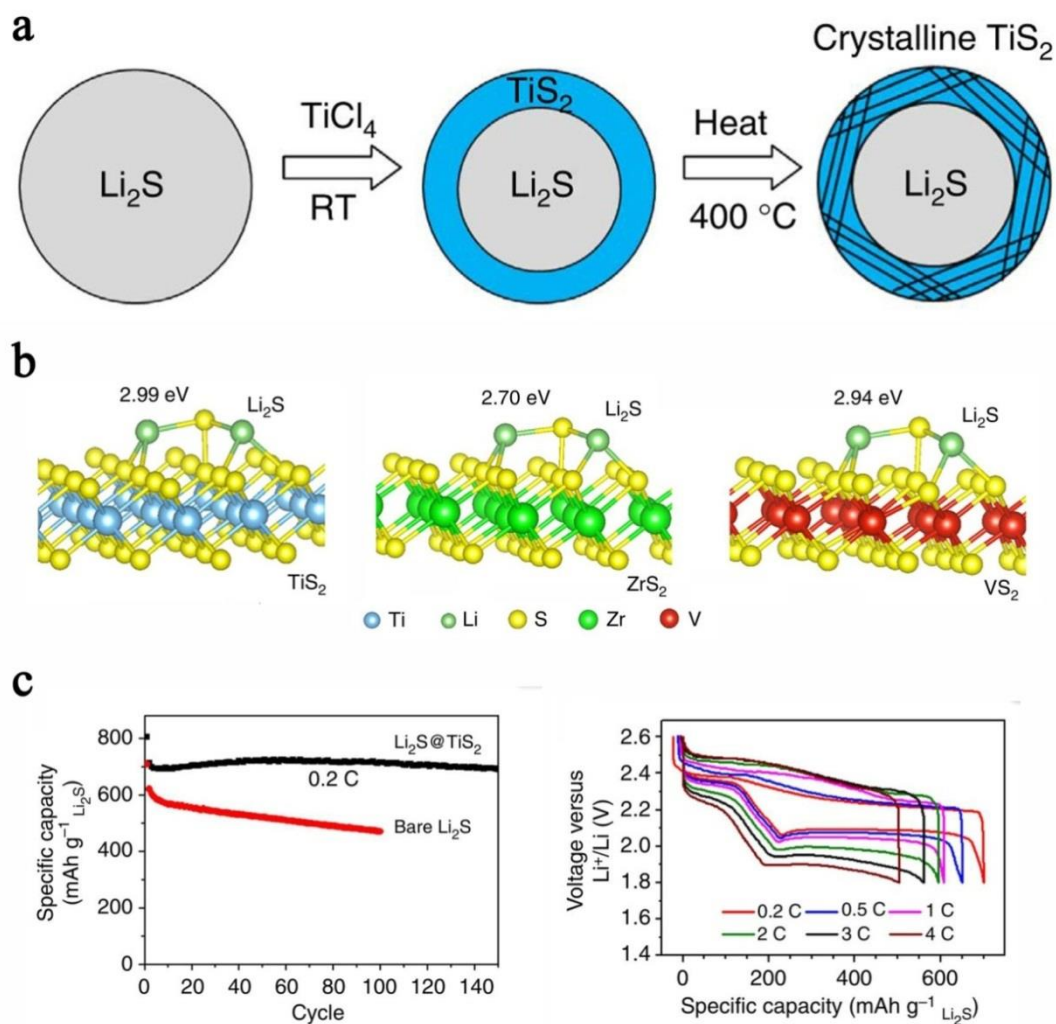


Figure 4. a) Binding geometries and energies of a Li_2S_4 molecule on graphene (left) and the (111) plane of CoS_2 with a cobalt-terminated surface (right). b) A schematic illustration of the discharge process in CoS_2 -incorporated carbon/sulfur cathode. c) Schematic illustration of the synthesis process for $\text{Co}_9\text{S}_8/\text{C-S}$ nanopolyhedra. d) Calculated adsorption energies (E_a) of S_8 and Li_2S_x ($x = 1, 2, 4, 6, \text{ or } 8$) species on (202) planes of Co_9S_8 crystals. e) Adsorption capability comparison of activated carbon (left vial) and $\text{Co}_9\text{S}_8/\text{C}$ hollow nanopolyhedra (right vial) within a solution of Li_2S_4 as a representative polysulfide (in mixed dioxolane (DOL)/dimethoxyethane (DME) solvent). a,b) Reproduced with permission.^[70] Copyright 2016, American Chemical Society. c-e) Reproduced with permission.^[71] Copyright 2017, Elsevier.



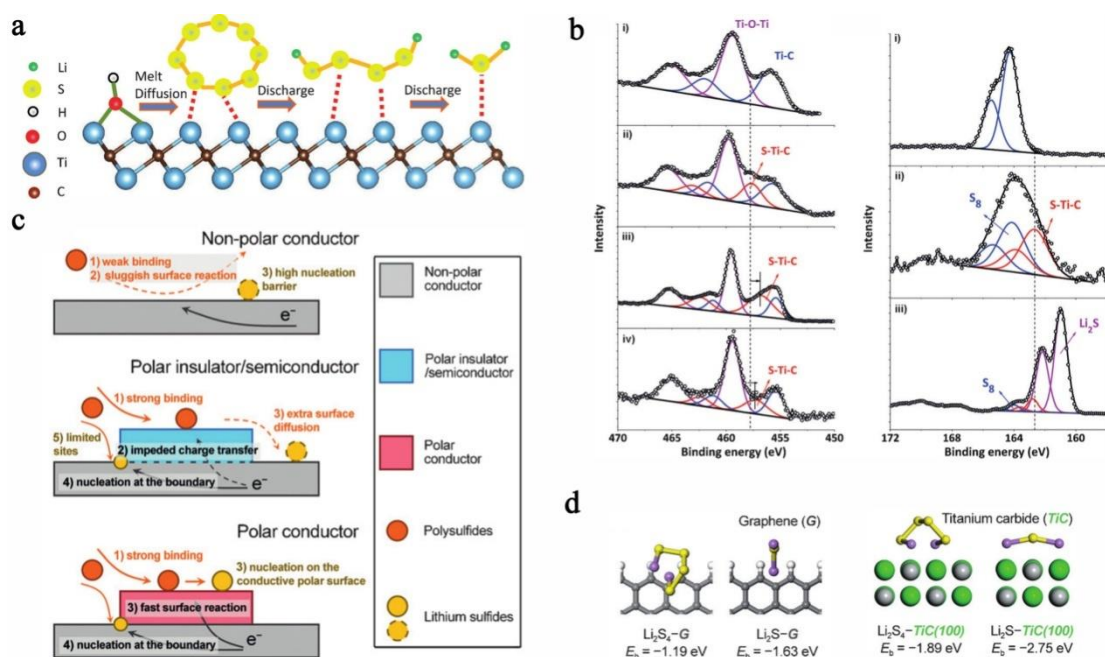


Figure 6. a) Geometry optimization of the interaction between Ti atoms on the surface of Ti₂C and sulfur species. (b) Ti 2p XPS spectrum (left) of i) Ti₂C nanosheets, ii) S/Ti₂C composite, iii) Li₂S₄-Ti₂C, and iv) 70S/Ti₂C electrodes discharged to 1.8 V; S 2p XPS spectra (right) of i) elemental sulfur, ii) 70S/Ti₂C composite, and iii) 70S/Ti₂C electrode discharged to 1.8 V. c) Illustration of the working mechanism of the polar conductor as it meets the demand for both adequate binding and charge transfer. d) The binding energies of TiC to Li₂S₄ and Li₂S compared to pristine graphene. a,b) Reproduced with permission.^[85] Copyright 2015, Wiley-VCH. c,d) Reproduced with permission.^[87] Copyright 2016, Wiley-VCH.

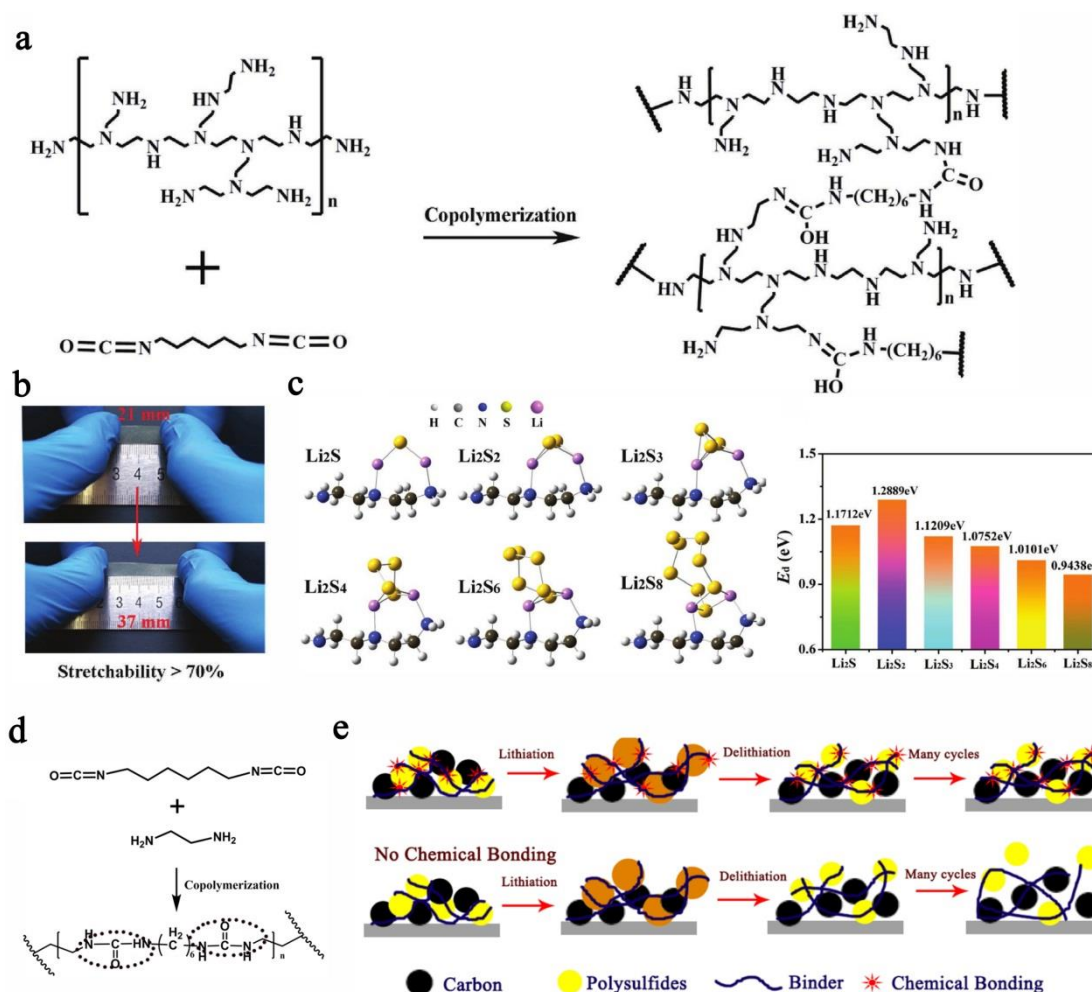


Figure 7. a) Synthesis scheme for AFG binder by copolymerization of PEI with HDI in DMF solution. b) Digital photographs show that the AFG copolymer has excellent stretchability. c) Adsorption binding energies for Li–S composites at six different lithiation stages on a reducible molecular structure of PEI. d) Synthesis scheme, in which AHP copolymerizes EDA with HDI in DMF solution. e) Schematic illustration of evolution of different binders during cycling. a-c) Reproduced with permission.^[89] Copyright 2017, Wiley-VCH. d) Reproduced with permission.^[91] Copyright 2017, Springer.

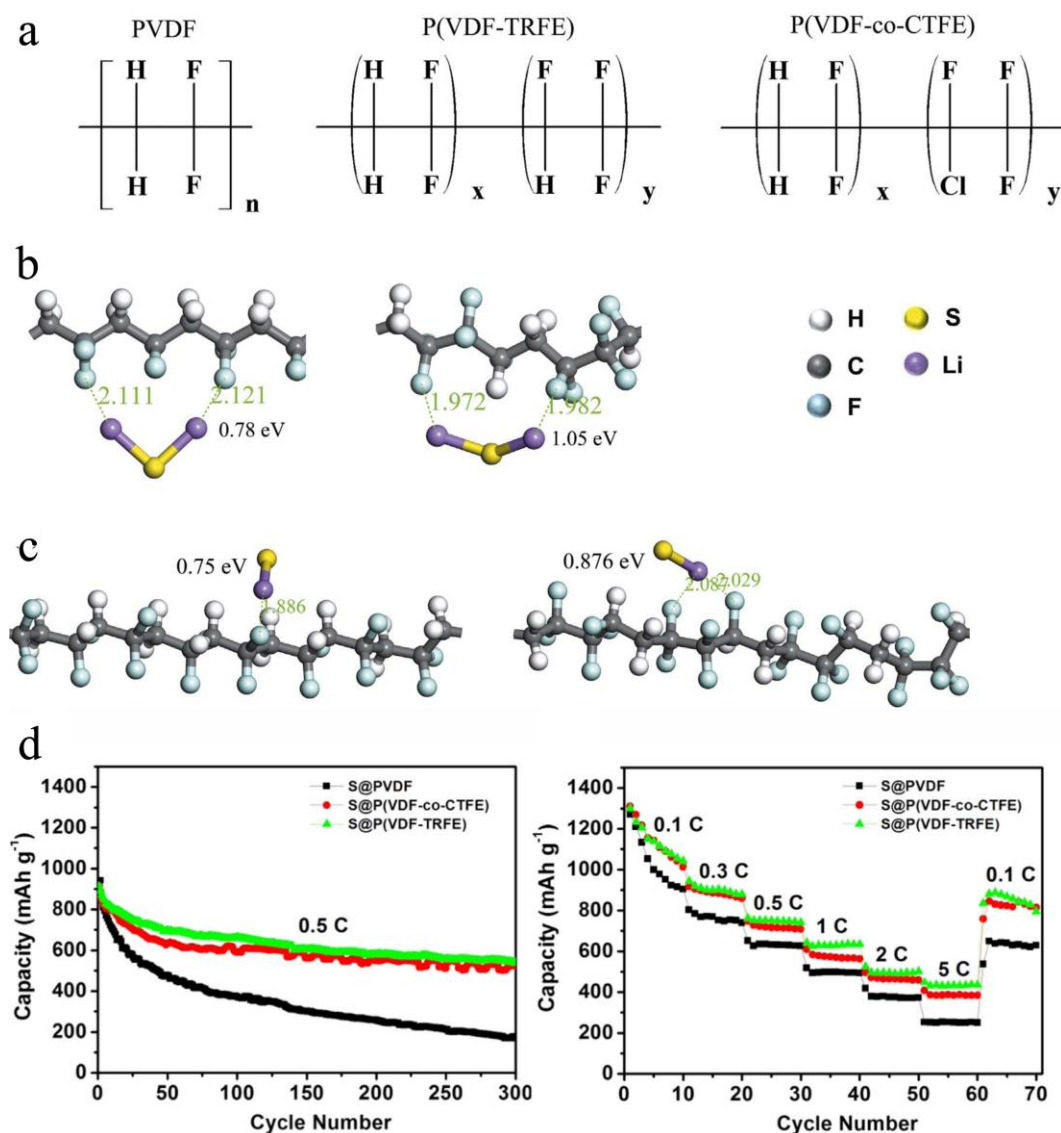


Figure 8. a) Chemical structures of PVDF, P(VDF-TRFE), and P(VDF-co-CTFE) binders; ab initio simulations showing the most stable binding configurations of (b) Li_2S and (c) Li-S species with PVDF (left) and P(VDF-TRFE) (right) binders. d) Long-term cycling performance (left) at 0.5 C and rate capability (right) of S@PVDF, S@P(VDF-co-CTFE), and S@P(VDF-TRFE) electrodes. a-d) Reproduced with permission.^[92] Copyright 2016, Elsevier.

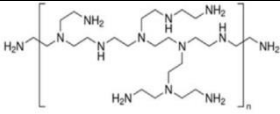
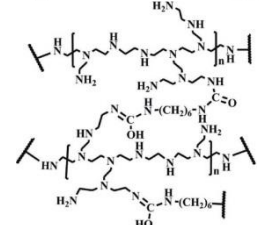
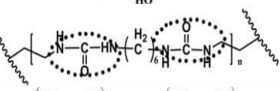
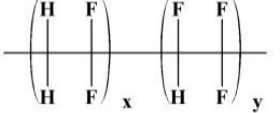
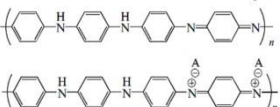
Table 1. Recent progress on polar inorganics as host materials in cathodes for lithium-sulfur batteries.

Polar inorganic host	Nanostructures	Sulfur content & sulfur loading mass ^{a)}	Binding energy	Cycling data ^{b)}	Ref.
TiO ₂	Yolk-shell	53 & 0.4-0.6	N/A	1030 (690)/1000 /0.5C	[36]
TiO ₂	Mesoporous spheres	49 & N/A	-2.31 (M3-HTSs) and -2.93 (M4-HTSs) eV between S _n ²⁻ with TiO ₂ (001) surface	801 (688)/200/0.5C	[38]
Nb ₂ O ₅	Nanocrystal with mesoporous carbon sphere	48 & 1.5	65.16 kcal mol ⁻¹ (equal to 2.82 eV) between Li ₂ S ₆ and Nb ₂ O ₅	1289 (913)/200/0.5C	[49]
δ-MnO ₂	Nanosheet	56 & 0.7-1.0	N/A	1120 (1030)/200/0.2C	[50]
MnO ₂	Nanosheet decorated hollow sulfur spheres	57 & 1.7-2.1	In the range of -3.86 to -5.15 eV between S _n ²⁻ species and MnO ₂ (100) surface	1043 (1072)/200/0.2C	[51]
Ti ₄ O ₇	Nanoparticles	48 & 1.5-1.8	N/A	850 (595)/500/2C	[58]
Co ₃ O ₄	Ultrathin nanosheets	42 & 0.6-1.0	5.58 eV between Li ₂ S and Co ₃ O ₄	890 (572)/300/0.6C	[63]
Ti ₄ O ₇	particles	51 & 0.5-1.5	-4 eV between Li ₂ S _x and Ti ₄ O ₇ (1-20)	623 (604)/250/0.5C	[59]
Ti ₆ O ₁₁	Nanowires	52 & 0.5-1.5	N/A	713 (635)/100/0.1C	[59]
CoS ₂	Micro-sized cluster with 15 wt% graphene	60 & 0.4	1.97 eV between Li ₂ S ₄ and (111) plane of CoS ₂	1368 (1005)/150 /0.5C	[70]
Co ₉ S ₈	Co ₉ S ₈ /C hollow nanopolyhedra	62 & 1.5 and 3.0	-6.08, -4.03, -2.97, -4.52, and -5.51 eV between Li ₂ S _x (x=8, 6, 4, 2, 1) and Co ₉ S ₈	1020 (790)/200/0.5C [1.5 mg cm ⁻²] 840 (680)/300/0.5C [3.0 mg cm ⁻²]	[71]
TiS ₂	Core-shell	51 & 1 (based on Li ₂ S)	2.99 eV between Li ₂ S and a single layer of TiS ₂	956 (736)/400/0.5C	[72]
MoS ₂	Nanosheet	N/A & 2	0.87 eV (2.70 eV, 4.48 eV) between Li ₂ S and MoS ₂ terrace site (S-, Mo-edge)	1068(over 800)/300/0.5C	[75]
Ti ₃ C ₂	Nanosheet with 10 wt% CNT	63 & 1.5 and 5.5	15.76 eV between Li ₂ S ₄ and Ti ₃ C ₂	1216 (450)/1200/0.5C [1.5 mg cm ⁻²] 916 (500)/250/0.2C [5.5 mg cm ⁻²]	[86]
TiC	Nanosheet with amount of graphene	55 & 3.5	-1.89 eV (-2.75 eV) between Li ₂ S ₄ (Li ₂ S) and TiC (100)	1032 (670)/100/0.2C	[87]

a) The sulfur content was calculated based on the weight of sulfur in the cathode and the unit is wt %. The unit of sulfur loading mass is mg cm⁻².

b) The cycling data are summarized as Initial (final) capacity/corresponding cycle number/corresponding current density. The specific capacity was calculated based on the weight of sulfur, and the unit of capacity is mAh g⁻¹.

Table 2. Polar organics employed as binders for lithium-sulfur batteries.

Polar organics	Chemical structure	Sulfur content & sulfur loading mass ^{a)}	Binding energy	Cycling data ^{b)}	Ref.
PEI binder		60 & 8.6	N/A	1126 (744)/50/0.05C	[88]
AFG binder		54 & 0.7, 3 and 8	1.2889 eV between Li ₂ S ₂ and AFG binder	600 (nearly 600)/600/1C [0.7 mg cm ⁻²] 614 (526)/200/0.5C [3 mg cm ⁻²] 988 (842)/50/0.1C [8 mg cm ⁻²]	[89]
AHP binder		51 & 0.5	N/A	773 (628)/100/1 C	[91]
P(VDF-TRFE) binder		42 & N/A	1.05 eV (0.876 eV) between Li ₂ S (Li-S [•] species) and P(VDF-TRFE)	912 (540)/300/0.5C	[92]
Polyaniline		59.8 & 0.6-0.9	N/A	872 (439)/50/0.07C	[93]

a) The sulfur content was calculated based on the weight of sulfur in the cathode, and the unit is wt %. The unit of sulfur loading mass is mg cm⁻².

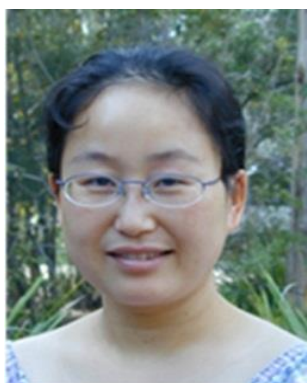
b) The cycling data are summarized as Initial (final) capacity/corresponding cycle number/corresponding current density. The specific capacity was calculated based on the weight of sulfur, and the unit of capacity is mAh g⁻¹.



Hongqiang Wang received his Ph.D. degree in 2016 from the Institute for Superconducting and Electronic Materials (ISEM) at the University of Wollongong. Since 2017, he has been a lecturer in the College of Chemistry and Environmental Science at Hebei University. His research topics focus on smart design and synthesis of nanostructured materials for high-performance lithium-sulfur and sodium-ion batteries.



Wenchao Zhang earned his B.S. and Master degrees in Materials Science and Engineering at the Central South University, PR China in 2012 and 2015, respectively. He is currently a Ph.D. candidate at the School of Mechanical, Materials, Mechatronics and Biomedical Engineering, University of Wollongong, Australia. His current research interests focus on the design and application of alloy-based anode materials for metal-ion batteries.



Zaiping Guo obtained her B.S. from the Department of Chemistry, Xinjiang University in 1993 and her Ph.D. from University of Wollongong in 2003. After her postdoctoral research with Prof. Huakun Liu at the Institute for Superconducting and Electronic Materials (ISEM), University of Wollongong, she joined the Faculty of Engineering in 2008. She is currently a senior professor of Faculty of Engineering & Information Sciences. Her work focuses on practical applications of various nanomaterials as electrode materials for energy storage or conversion technologies, including rechargeable batteries, hydrogen storage, and supercapacitors.

The importance of the strong chemical interaction between polar materials and polysulfides has been recognized by researchers to improve the performance of Li-S batteries, especially with respect to the shuttle effect. Recent advances in polar materials for Li-S batteries are reviewed, including polar inorganic and polar organic materials. Also, future directions and prospects for polar materials used in Li-S batteries are proposed.

Keywords: lithium-sulfur batteries; polar inorganics; polar organics; chemical interaction.

Hongqiang Wang^{a,b,c}, Wenchao Zhang^b, Jianzhong Xu^a, Zaiping Guo^{b*}

Advances in Polar Materials for Lithium-Sulfur Batteries

